

Language-guided Medical Image Segmentation with Target-informed Multi-level Contrastive Alignments

Mingjian Li^{a, b, †}, Mingyuan Meng^{a, b, †}, Shuchang Ye^a, Michael Fulham^{a, c},
Lei Bi^{a, b, *}, and Jinman Kim^{a, *}

^a School of Computer Science, The University of Sydney, Australia.

^b Institute of Translational Medicine, Shanghai Jiao Tong University, China.

^c Department of Molecular Imaging, Royal Prince Alfred Hospital, Australia.

Abstract — Medical image segmentation is a fundamental task in numerous medical engineering applications. Recently, language-guided segmentation has shown promise in medical scenarios where textual clinical reports are readily available as semantic guidance. Clinical reports contain diagnostic information provided by clinicians, which can provide auxiliary textual semantics to guide segmentation. However, existing language-guided segmentation methods neglect the inherent pattern gaps between image and text modalities, resulting in sub-optimal visual-language integration. Contrastive learning is a well-recognized approach to align image-text patterns, but it has not been optimized for bridging the pattern gaps in medical language-guided segmentation that relies primarily on medical image details to characterize the underlying disease/targets. Current contrastive alignment techniques typically align high-level global semantics without involving low-level localized target information, and thus cannot deliver fine-grained textual guidance on crucial image details. In this study, we propose a Target-informed Multi-level Contrastive Alignment framework (TMCA) to bridge image-text pattern gaps for medical language-guided segmentation. TMCA enables target-informed image-text alignments and fine-grained textual guidance by introducing: (i) a target-sensitive semantic distance module that utilizes target information for more granular image-text alignment modeling, (ii) a multi-level contrastive alignment strategy that directs fine-grained textual guidance to multi-scale image details, and (iii) a language-guided target enhancement module that reinforces attention to critical image regions based on the aligned image-text patterns. Extensive experiments on four public benchmark datasets, involving three medical imaging modalities paired with corresponding clinical reports, demonstrate that TMCA enabled superior performance over state-of-the-art language-guided medical image segmentation methods.

Keywords — Medical Image Segmentation, Language-guided Segmentation, Contrastive Alignment.

1. Introduction

Medical image segmentation is a fundamental task in numerous medical engineering applications, including computer-aided diagnosis, radiation therapy planning, and surgical navigation [1]. The aim of medical image segmentation is to identify regions of interest (ROIs) in medical images, e.g., identifying and quantifying tumor ROIs in cancer patient scans is a key factor in determining disease progression and the effectiveness of treatment [2]. In recent years, deep learning-based methods have achieved notable success for automatic medical image segmentation [3, 4, 5]. While early segmentation methods typically focused on exploiting image information, leveraging textual clinical reports as complementary information for segmentation has gained wide attention for its potential to transcend the performance bounds of image-only segmentation methods. Clinical reports, formulated by clinical experts, are readily available with the images and can provide valuable semantic information, including diagnostic imaging findings and interpretations. Recently, language-guided segmentation methods, which leverage auxiliary textual semantics in clinical reports to guide segmentation, have emerged to boost segmentation performance [6, 7, 8, 9].

[†] M. Li and M. Meng contributed equally to this work.

* Corresponding authors: lei.bi@sjtu.edu.cn (Lei Bi) and jinman.kim@sydney.edu.au (Jinman Kim).

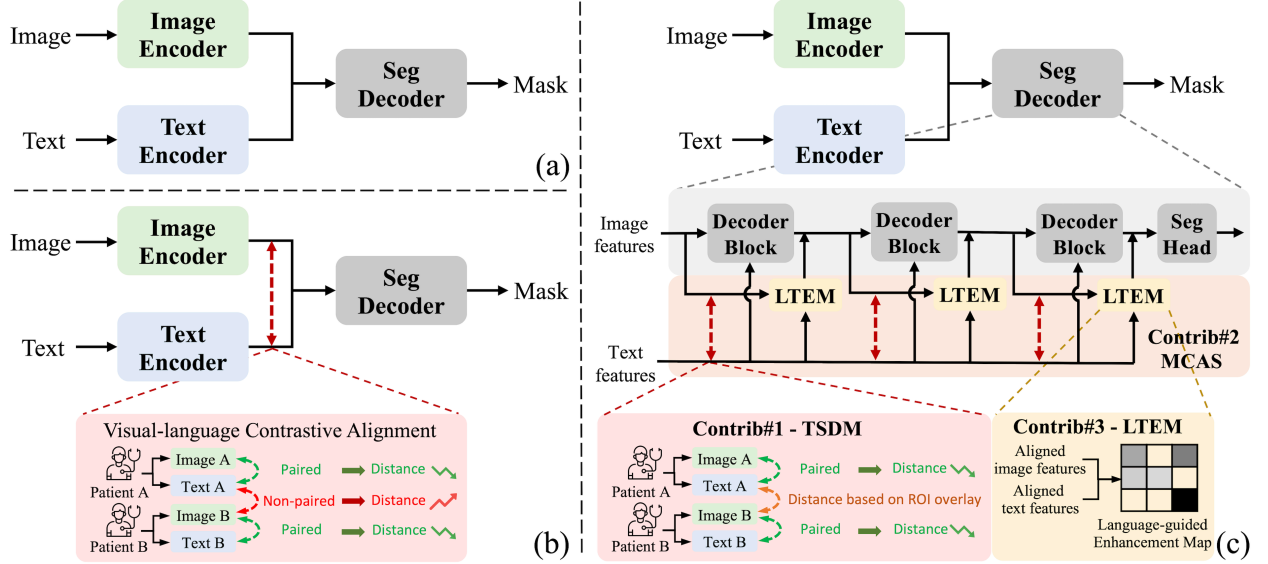


Figure 1. Illustration of (a) language-guided segmentation that directly integrates image and text features, (b) language-guided segmentation enhanced by visual-language contrastive alignments, and (c) the proposed Target-informed Multi-level Contrastive Alignment framework (TMCA) for language-guided segmentation, featuring three technical contributions: Target-sensitive Semantic Distance Module (TSDM, Contrib#1), Multi-level Contrastive Alignment Strategy (MCAS, Contrib#2), and Language-guided Target Enhancement Module (LTEM, Contrib#3).

Language-guided medical image segmentation methods typically extract image and text features using separate encoders and integrate them via direct visual-language feature fusion (Figure 1a), exploiting textual semantic guidance with visual contexts [7, 8]. However, despite the improved segmentation performance, these methods neglect the pattern gaps between image and text modalities during feature fusion, resulting in sub-optimal information integration and less-effective textual guidance. This is because image and text modalities are inherently encoded in different patterns: images are continuous and rich in details, whereas text is discrete and concise with a focus on high-level concepts. Moreover, the encoders used for extracting image and text features are fundamentally different, further enlarging the pattern gaps between the extracted image and text features.

Vision-language contrastive learning can bridge image-text pattern gaps by associating the semantics of paired image-text features through contrastive alignments [10, 11]. In language-guided segmentation, standard contrastive alignment can be used to align the image and text features before feature fusion (Figure 1b), which attempts to minimize the semantic distance between paired image-text features (from the same patient) while maximizing the semantic distance between non-paired features (from different patients). Unfortunately, this straightforward adoption does not optimize contrastive alignment for medical image segmentation and, therefore, leaves considerable research gaps. Existing contrastive alignments typically align global image-text semantics holistically, favoring vision tasks related to global semantics (such as image classification); however, segmentation aims to delineate local ROIs in medical images, making it a localized task instead of characterizing the entire image. This conflict incurs limitations specifically in two ways: (i) First, current contrastive alignment techniques have no awareness of ROI target information and assume exact correspondence between paired image-text features (i.e., assume that they are from the same patient) [10], facing challenges when aligning image-text pairs from different patients that, while not identical in holistically, have similar ROIs. Consequently, there may be under-alignment between image-text features that are semantically related but derived from different patients, and this might disrupt the feature alignment process and lead to poor feature fusion. (ii) Second, medical image segmentation, as a pixel-wise prediction task, relies primarily on subtle low-level image details to characterize the underlying disease/targets and identify the ROI boundaries [50]. However, current contrastive alignment techniques typically align high-level semantics only at the deepest level of encoders, thereby preventing the delivery of fine-grained textual guidance directly on subtle medical image details.

In this study, we propose TMCA, a novel Target-informed Multi-level Contrastive Alignment framework particularly designed to bridge the image-text pattern gaps for language-guided medical image segmentation. As illustrated in Figure 1c, our TMCA incorporates ROI target information into image-text alignment modeling and directs fine-grained textual guidance to crucial medical image details, featuring three technical contributions as follows:

- Target-sensitive Semantic Distance Module (TSDM) calculates semantic distance based on the intersection ratios of ROIs, thus enabling alignments between image-text features that describe similar ROIs but differ in less-important backgrounds.
- Multi-level Contrastive Alignment Strategy (MCAS) performs contrastive alignments at multiple feature pyramid levels, hence delivering fine-grained textual guidance on multi-scale image features containing rich image details.
- Language-guided Target Enhancement Module (LTEM) reinforces attention to critical image regions by explicitly associating the aligned image-text features with target-related image sub-regions.

Extensive experiments were conducted on four public benchmark datasets across three medical image modalities, including X-ray (QaTa-COV19 [12]), computed tomography (MosMedData [13]), and endoscopic images (Kvasir-SEG [14] and Bkai-polyp [15]). The experimental results showed that our TMCA consistently outperformed state-of-the-art language-guided medical image segmentation methods across all four evaluation datasets, underscoring its generalizability and effectiveness.

2. Related Work

2.1. Deep Learning for Medical Image Segmentation

Deep learning has made substantial advances in medical image segmentation. The U-Net [16] using a convolution neural network (CNN) has demonstrated outstanding performance for biomedical image segmentation, whose U-shaped architecture is composed of a contracting encoder for contextual understanding and a symmetric expanding decoder for ROI delineation. This architecture has been shown to be instrumental in learning multi-scale feature representations for precise segmentation. U-Net++ [17] then re-vamped skip connections to mitigate the semantic gaps between the encoder and decoder. Attention U-Net [18] introduced attention gates to suppress non-target backgrounds. Swin UNETR [19] introduced transformers with shifted windows to capture long-range contexts across image sub-regions. Meanwhile, Isensee et al. [20] proposed nnU-Net to automate the optimal configuration process of U-Net. Ma et al. [21, 22] proposed a foundation segmentation model, MedSAM, trained on large-scale medical data and demonstrated great generalizability across datasets. Furthermore, segmentation methods using multi-modal medical images are gaining prominence over single-modal methods. Kamnitsas et al. [23] proposed a segmentation model that combines multiple CNNs, each trained on different medical imaging modalities. Guo et al. [24] investigated three distinct strategies for integrating multi-modal medical images, noting that fusing multi-modal information within the network contributed to superior performance when compared to outcome-level fusion (e.g., majority voting). Although deep learning has made impressive advances in medical image segmentation, its success is greatly reliant on the availability of large-scale labeled training data, which are usually tedious and time-consuming to annotate and difficult to acquire due to various ethical constraints [25].

2.2. Language-guided Medical Image Segmentation

To exploit readily available textual clinical reports to improve segmentation accuracy, language-guided segmentation methods have emerged and shown promising performance. For instance, Tomar et al. [9] extracted textual semantics via ‘byte-pair’ encoding and employed it as soft channel attention to reinforce critical image features. Li et al. [6] proposed LViT that integrated image and text features using a U-shaped CNN alongside a U-shaped Visual Transformer (ViT) [26]. These methods extracted text features via simple vectorization operations, incurring difficulties in capturing rich textual semantics. To mitigate this, Lee et al. [8] employed the text encoder of CLIP [27], which was pretrained on a large language corpus and had proven effective for various textual tasks for feature extraction, and then integrated the extracted text features with image features via cross-attention. To further accommodate

various medical concepts and specialized knowledge in clinical reports, Zhong et al. [7] employed a medical domain-specific text encoder, CXR-BERT [31], to extract text features encoded with rich semantics and then fuse them with image features. Hu et al. [28] proposed to extract image features from the pretrained Segment Anything Model (SAM) [29] and integrated them with text features extracted from the pretrained BERT [30] model for segmentation. Recently, Huang et al. [32] proposed a cross-modal conditioned reconstruction model (RecLMIS) for medical language-guided segmentation, which explicitly captured image-text interactions by conditioned vision-language reconstruction. These methods focused on enhancing segmentation accuracy with textual semantics and required textual reports as input during both training and inference. To alleviate the reliance on textual input, Ye et al. [33, 34] performed joint report generation or leveraged prototype learning to generate textual semantics for inference without necessitating textual reports as input. Unfortunately, these methods compromised the segmentation accuracy compared to common language-guided segmentation methods that require textual reports during inference.

Most language-guided medical image segmentation methods focused on feature extraction and fusion strategies to establish image-text semantic interactions, but neglected the inherent pattern gaps between the two distinct image and text modalities. Only a few studies attempted to bridge the pattern gaps in language-guided segmentation. For example, Pan et al. [35] adopted evidential learning to bridge the pattern gaps by measuring the modality gap based on opinion aggregation; Zhou et al. [36] adopted contrastive learning to holistically align the features of image and text encoders via a multi-stage cross-modality contrastive loss. These methods alleviate the image-text pattern gaps via established evidential/contrastive learning techniques; however, they failed to tailor the techniques for language-guided segmentation tasks, e.g., incorporating ROI target information into alignment modeling.

2.3. Contrastive Alignment

Vision-language contrastive learning is a widely used technique that learns the general image representations from language supervision, where text acts as “pseudo instance-level classification labels”. CLIP [27] is a pioneering work that involved over 400 million image-text pairs. Zhang et al. [10] introduced contrastive learning to the medical imaging domain, which minimized the distance between paired image-text features from the same patient while maximizing the distance between non-paired features from different patients. Also, Huang et al. [37] proposed joint global-local contrastive representation learning, Wang et al. [38] further explored multi-granularity feature alignment, and Li et al. [39] proposed to model image-text inter-match relations. Once pretrained, the image encoder can be applied to various downstream tasks using task-specific decoders, such as classification, detection, and segmentation [11]. However, this pretraining-based approach cannot explicitly extract and leverage textual semantics for inference. Therefore, in this study, we explored a different approach toward contrastive image-text alignment tailored for segmentation: the contrastive alignments are deeply embedded into the segmentation decoder, so that the whole encoder-decoder framework can jointly learn and collectively infer for segmentation with better utilization and integration of image-text features.

In addition, medical images and reports of different patients can have large semantic similarities, e.g., describing similar diseases. Recently, Wang et al. [40] proposed to measure alignment distance based on disease classification labels, and Liu et al. [41] also proposed to use text feature similarities for semantically-aware alignment distance measurement. However, these methods were not applicable to segmentation tasks: for example, the disease labels could be the same for different patients, while the ROI locations and shapes vary substantially. To the best of our knowledge, our TMCA is the first contrastive alignment framework tailored for language-guided segmentation, focusing on localized, target-sensitive alignment for clinically-critical ROIs.

3. Method

The overall architecture of our TMCA is illustrated in Figure 2, which consists of image/text encoders (detailed in Section 3.1) and a segmentation decoder equipped with target-informed multi-level contrastive alignments (detailed in Section 3.2). The decoder part contains our three technical contributions: TSDM (Section 3.2.1), MCAS (Section 3.2.2), and LTEM (Section 3.2.3).

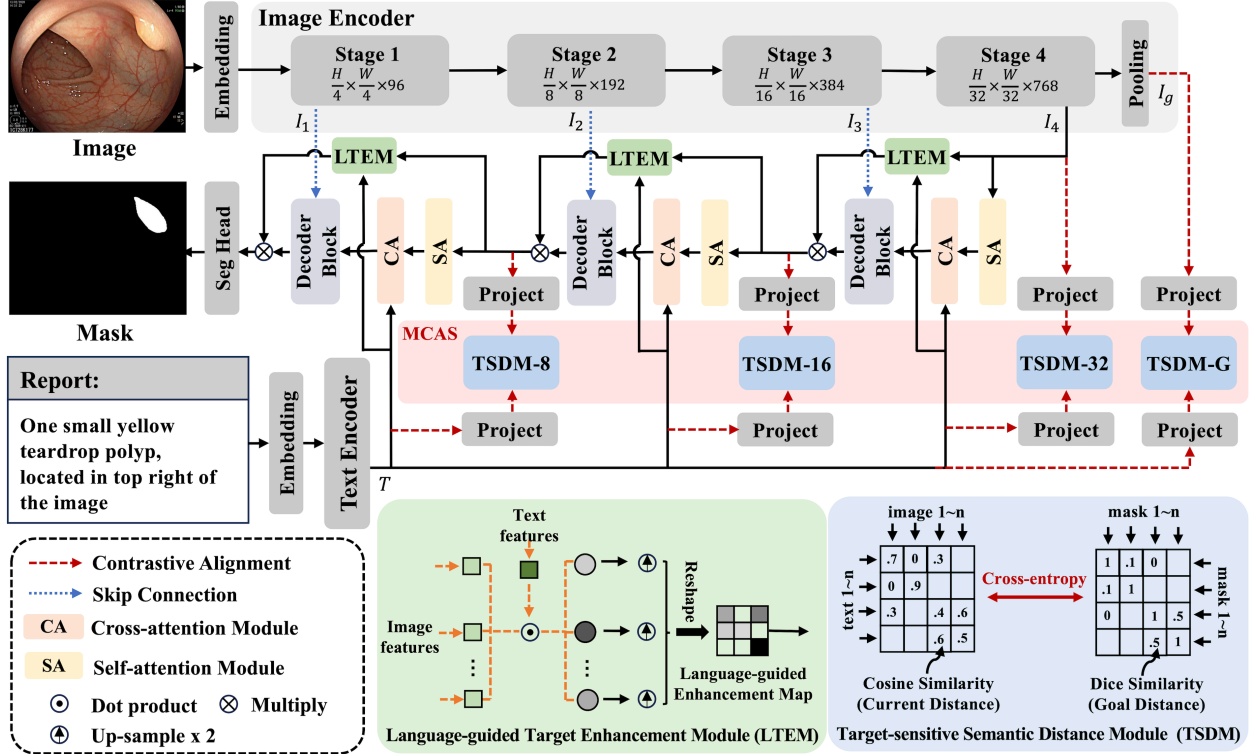


Figure 2. Overall architecture of our TMCA for language-guided medical image segmentation, containing image/text encoders and a segmentation decoder with target-informed multi-level contrastive alignments.

3.1. Image and Text Encoders

ConvNeXt-Tiny [42] was used as the image encoder following Zhong et al. [7], where multi-scale image features were extracted from four stages of the image encoder, denoted as $[I_1, I_2, I_3, I_4]$. We also extract global image features using a global pooling layer after the last stage of the image encoder, which is denoted as I_g .

CXR-BERT [31], a medical domain-specific language model, was employed as the text encoder. CXR-BERT was pretrained on large-scale medical reports and has shown great capability in textual semantics extraction. We extract text features from the last three layers of CXR-BERT, and then average them to derive the final text features T .

3.2. Segmentation Decoder with Target-informed Multi-level Contrastive Alignments

The segmentation decoder progressively integrates features from the image and text encoders, which consists of three successive decoder blocks followed by a segmentation head that projects the final feature maps into segmentation masks. The segmentation loss is defined as the sum of Dice Loss and Cross-Entropy Loss.

Before each decoder block, the input image and text features are semantically aligned via contrastive alignments based on our Target-sensitive Semantic Distance Module (TSDM, detailed in Section 3.2.1). In addition to the TSDM modules used before the three decoder blocks, another TSDM module is used to align the global semantics between I_g and T , totaling four levels of contrastive alignments in our Multi-level Contrastive Alignment Strategy (MCAS, detailed in Section 3.2.2).

Within each decoder block, the TSDM-aligned image features with a positional embedding are fed into a multi-head self-attention (SA) module to capture long-range intra-modal relations, followed by a multi-head cross-attention (CA) module to integrate the SA-output image features with the TSDM-aligned text features (image features serve as Q and text features serve as K/V). Both the SA

and CA modules have shortcut connections between their inputs and outputs. After that is a standard U-Net upsample block with a skip connection from the image encoder; specifically, a deconvolution layer upsampled the feature maps by a factor of 2, followed by two convolution layers to integrate the image features propagated from the skip connection.

After each decoder block, a Language-guided Target Enhancement Module (LTEM, detailed in Section 3.2.3) is used to exploit the aligned image-text semantics to guide attention to critical image regions. The output features of the decoder block are gated by the language-guided enhancement map produced by LTEM and then passed into the next decoder block.

3.2.1 Target-sensitive Semantic Distance Module (TSDM)

Our TSDM enables segmentation-tailored contrastive alignment to bridge the pattern gaps between image and text features. Common contrastive alignment techniques attempt to minimize the semantic distance between paired image-text features from the same patient, while maximizing the semantic distance between non-paired features from different patients. The underlying assumption is that the paired image and text should have identical semantics (otherwise they are regarded as “unpaired”). However, similarities between medical images and text have multi-granularity properties [38]. For example, images and text from different patients with the same disease could have similar semantics. Therefore, our contrastive alignment modeling is more granular, where the images and text from different patients can also be “paired” if they correspond to similar ROI targets.

As segmentation masks clearly delineate the target-related image regions that contain critical semantics, the semantic distance between different patients can be measured based on the intersections of their corresponding segmentation masks. Specifically, in the construction of contrastive alignment goals, the semantic distance $d_{p,q}$ for the p -th image and the q -th text in the batch is defined by the Dice coefficient between their corresponding ground truth segmentation masks. SoftMax is then applied to normalize $d_{p,q}$ across the batch dimension with a temperature τ_1 . Similarly, the current cosine distance $s_{p,q}$ between the p -th image features and the q -th text features in the batch is calculated and normalized using SoftMax with a temperature τ_2 .

A target-sensitive semantic contrastive loss is employed as the objective function of TSDM, calculated as a cross-entropy loss between the current distance $s_{p,q}$ and the target semantic distance $d_{p,q}$:

$$L = -\frac{1}{Bz} \sum \sum d_{p,q} * \log(s_{p,q}), \quad (1)$$

where Bz is the batch size. In our implementation, we computed the semantic contrastive loss in both image-to-text and text-to-image directions and then averaged them to derive a bi-directional contrastive loss.

3.2.2 Multi-level Contrastive Alignment Strategy (MCAS)

Our MCAS performs contrastive alignments at multiple feature pyramid levels, which delivers fine-grained textual guidance on multi-scale image features containing rich low-level image details as well as global image features I_g containing high-level image semantics. Specifically, the contrastive alignments conducted before three decoder blocks are denoted as TSDM-8/16/32, where the text features T are semantically aligned with the image features in 1/8, 1/16, and 1/32 scales, respectively. Also, a global contrastive alignment, denoted as TSDM-G, is applied to align the global semantics between the global image features I_g and the text features T . The text features T are projected to match the dimension of image features at each level through linear projection. The final loss for multi-level contrastive alignments is defined as the average of bi-directional contrastive losses across all four levels.

3.2.3 Language-guided Target Enhancement Module (LTEM)

Our LTEM leverages the aligned image-text features to highlight critical image regions. Since the deeper layers of CNNs tend to contain high-level semantic information, while the shallower layers tend to contain low-level detail information [43], we calculate a language-guided cross-attention map based on high-level image-text features to gate the low-level image features output from

decoder blocks. Specifically, we calculate the normalized dot product similarity between the i -th image sub-region features I_i and the global text features T_g (i.e., globally pooling T across the word length), which is defined as:

$$w_i = I_i^T T_g. \quad (2)$$

Then, we normalize w_i across the image sub-region dimension using SoftMax with a temperature τ_3 . The normalized map is reshaped and upsampled by a factor of 2, resulting in a language-guided enhancement map. Finally, the enhancement map is multiplied by the decoded image features, which is then passed into the next decoder block or the final segmentation head.

4. Experimental Setup

4.1. Datasets and Preprocessing

We evaluated our method on four well-established public benchmark datasets, QaTa-COV19 [12], MosMedData [13], Kvasir-SEG [14], and Bkai-polyp [15], involving X-ray, computed tomography (CT), and endoscopic images paired with textual reports.

The QaTa-COV19 dataset contains 9258 COVID-19 Chest X-rays with ground-truth segmentation labels for the COVID-19 infected regions. The official training set of the QaTa-COV19 dataset contains 7145 samples, while the test set contains 2113 samples. Following the preprocessing procedure in Zhong et al.’s work [7], the official training set was split into train and validation sets with a distribution of 80% and 20%. The MosMedData dataset contains 2729 CT slices depicting pulmonary infections with ground truth segmentation labels. We followed the preprocessing procedure in Li et al.’s work [6], splitting the dataset into 2183, 273, and 273 samples for training, validation, and testing. For language-guided segmentation, Li et al. [6] extended the QaTa-COV19 and MosMedData datasets with matched textual reports. Each report contains three sentences: the first sentence indicates the presence of infection, the second outlines the number of involved regions, and the third describes their location, which provide rich semantics that can be used to guide the lesion segmentation.

The Kvasir-SEG and Bkai-polyp datasets, respectively, contain 1000 endoscopic images with ground-truth segmentation labels of gastrointestinal polyps. We followed the preprocessing procedure in Poudel et al.’s work [44], splitting the datasets with a ratio of 8:1:1 for training, validation, and testing. Poudel et al. [44] also extended these two datasets with matched textual reports, describing the polyp size, number, color, and location in a free-text format.

4.2. Implementation Details

The deep learning models were trained using a Nvidia 24 GB RTX3090 GPU with a batch size of 32. PyTorch was employed with PyTorch Lightning as the wrapper for training and testing. The AdamW optimizer was used with a learning rate set to 3e-4, and a cosine annealing scheduler was employed with the minimal learning rate set to 1e-6. All images were resized to a dimension of 224×224. Image augmentation was applied by a random zoom with a 10% probability.

4.3. Experimental Settings

Our TMCA was extensively compared against state-of-the-art methods for medical image segmentation in three categories: (i) image-only segmentation methods including U-Net [16], U-Net++ [17], nnU-Net [20], and Attention U-Net [18]; (ii) vision-language pretraining (VLP)-based methods including CLIP [27] and GloRIA [37]; (iii) language-guided segmentation methods including LViT [6], TGANet [9], Ariadne [7], RecLMIS [32], EviVLM [35], and HCFNet [36].

Moreover, two ablation studies were conducted to investigate (i) the individual effectiveness of our three technical contributions, and (ii) the effects of applying different levels of contrastive alignments in MCAS. A baseline segmentation model was built for comparison in the ablation studies, which has the same encoder-decoder architecture as ours but removes all the components related to our target-informed multi-level contrastive alignments.

We adopted two commonly used segmentation evaluation metrics: Dice Similarity Coefficient (Dice) and mean Intersection over Union (mIoU), two widely recognized metrics for measuring spatial overlap between the predicted and ground truth segmentation masks. In general, a higher Dice or a higher mIoU indicates a better segmentation performance.

5. Results

5.1. Comparison with Existing Methods

Table 1 presents a quantitative comparison with existing methods for medical image segmentation. Language-guided methods achieved better overall performance than image-only and VLP-based methods, while VLP-based methods failed to outperform image-only methods despite using textual information during pretraining. Among language-guided methods, HCFNet outperformed other recently proposed methods (RecLMIS and EviVLM), achieving the second-best performance. Nevertheless, our TMCA still outperformed HCFNet, especially by a large margin on the Kvasir-SEG and Bkai-polyp datasets.

Moreover, most comparison methods exhibited inconsistent performance across four datasets. Among image-only methods, U-Net++ achieved the best performance on the QaTa-COV19 and Bkai-polyp datasets, while nnU-Net and Attention U-Net achieved the best performance on the MosMedData and Kvasir-SEG datasets, respectively. For language-guided methods, Ariadne achieved the second-best Dice result on the Bkai-polyp dataset, but its results on the other datasets are worse than HCFNet. Similarly, EviVLM achieved the second-best mIoU result on the MosMedData dataset, but its results on the QaTa-COV19 and Bkai-polyp datasets are even worse than Ariadne. In contrast, our TMCA achieved the best performance consistently across all evaluation datasets.

Figure 3 shows a qualitative comparison with existing methods for medical image segmentation, demonstrating that our TMCA accurately segmented lesions even in cases of low image contrast and image quality (rows 1, 2, 3, and 5). Other methods, especially image-only methods (U-Net and U-Net++), tended to produce false positive segmentation results (rows 1-7) and/or failed to segment lesions with low contrast to the background (rows 2, 5, and 6). Other language-guided methods (LViT and Ariadne) used textual guidance to reduce false positive results (e.g., row 1, where the text specified that there is no infected region in left lung) and to segment challenging regions (e.g., row 6, where the text indicates that there is polyp at the top of the image). Nevertheless, our TMCA further refined the textual guidance through the proposed TSDM and applied it to subtle image details through the proposed MCAS and LTEM, achieving the most accurate segmentation results across all four datasets.

Table 1. Quantitative comparison between our TMCA and existing methods for medical image segmentation.

Method	QaTa-COV19		MosMedData		Kvasir-SEG		Bkai-polyp	
	mIoU (%)	Dice (%)						
Image-only								
U-Net [16]	70.92	82.99	50.73	64.60	69.62	82.09	79.06	88.31
U-Net++ [17]	71.96	83.69	58.39	71.75	69.58	82.06	79.87	88.81
nnU-Net [20]	70.81	80.42	60.36	72.59	-	-	-	-
Attention U-Net [18]	70.06	82.40	52.82	66.34	74.19	85.18	72.97	84.26
VLP-based								
CLIP [27]	70.66	79.81	59.64	71.97	-	-	-	-
GloRIA [37]	70.68	79.94	60.18	72.42	-	-	-	-
Language-guided								
LViT [6]	73.79	84.92	61.33	74.57	77.04	87.03	75.19	85.84
TGANet [9]	70.75	79.87	59.28	71.81	83.30	89.82	84.09	90.23
Ariadne [7]	81.45	89.78	63.04	77.33	80.70	89.32	88.02	93.63
RecLMIS [32]	77.00	85.22	65.07	77.48	78.76	85.75	78.42	88.63
EviVLM [35]	77.34	85.79	<u>65.81</u>	77.64	82.45	89.63	85.25	90.76
HCFNet [36]	<u>83.06</u>	<u>90.75</u>	65.75	<u>79.34</u>	<u>83.49</u>	<u>90.18</u>	<u>88.10</u>	93.14
TMCA (Ours)	83.27	90.87	65.94	79.56	85.54	92.20	89.91	94.69

Bold/Underline: The best/second-best result in each column.

Image	Text	Ground Truth	U-Net (Image-only)	U-Net++ (Image-only)	LViT (Language-guided)	Ariadne (Language-guided)	TMCA (Language-guided)
	Unilateral pulmonary infection, one infected area, right lung						
	Unilateral pulmonary infection, one infected area, middle right lung						
	Unilateral pulmonary infection, one infected areas, middle left lung						
	Unilateral pulmonary infection, one infected area, middle right lung						
	one medium white heart polyp, located in right of the image						
	Two large white round polyp, located in top left, top of the image						
	one small brown oval polyp, located in top right of the image						
	One medium white circle polyp, located in right of the image						

Figure 3. Qualitative comparison with existing methods for medical image segmentation on the QaTa-COV19 (rows 1-2), MosMedData (rows 3-4), Kvasir-SEG (rows 5-6), and Bkai-polyp (rows 7-8) datasets. Red boxes indicate the regions falsely identified (false positive) and blue boxes indicate the regions not identified (false negative).

5.2. Ablation Analysis of Each Component

Table 2 presents our first ablation study, where our three technical contributions (MCAS, LTEM, and TSDM) were incrementally added to the baseline segmentation model. Initially, adding MCAS led to the largest performance improvement, with an increase of 2.71/1.64% in mIoU/Dice over the baseline model. Subsequently, adding LTEM and TSDM further improved segmentation performance, eventually resulting in an increase of 4.84/2.88% in mIoU/Dice over the baseline model.

Table 2. Ablation results of incrementally adding each component on the Kvasir-SEG dataset.

TSDM	LTEM	MCAS	mIoU (%)	Dice (%)	Accuracy (%)
×	×	×	80.70	89.32	97.12
×	×	✓	83.41	90.96	97.46
×	✓	✓	<u>84.58</u>	<u>91.64</u>	<u>97.65</u>
✓	✓	✓	85.54	92.20	97.82

Bold/Underline: The best/second-best result in each column.

5.3. Ablation Analysis on Multi-level Contrastive Alignments

Table 3 presents our second ablation study, where different levels of target-informed contrastive alignments (with TSDM and LTEM) were added to the baseline segmentation model. We noticed that adding TSDM-G to align global image-text semantics has yielded an increase of 1.60/0.91% in mIoU/Dice over the baseline model, while adding TSDM at 1/32, 1/16, and 1/8 scales (TSDM-32/16/8) further improved segmentation performance, eventually resulting in an increase of 4.84/2.88% in mIoU/Dice.

Table 3. Ablation results of multi-level contrastive alignments on the Kvasir-SEG dataset.

Method	mIoU (%)	Dice (%)	Accuracy (%)
Baseline	80.70	89.32	97.12
+ TSDM-G	82.30	90.23	97.29
+ TSDM-G/32	83.74	91.14	97.55
+ TSDM-G/32/16	<u>84.35</u>	<u>91.51</u>	<u>97.63</u>
+ TSDM-G/32/16/8	85.54	92.20	97.82

Bold/Underline: The best/second-best result in each column.

6. Discussion

Through extensive experimental validation, our study reveals three main findings: (i) Our TMCA outperformed state-of-the-art medical image segmentation methods and exhibited great generalizability across various imaging modalities and segmentation tasks; (ii) The proposed TSDM, LTEM, and MCAS collectively enhanced the segmentation performance by enabling finer-grained textual semantic guidance on critical image regions; (iii) Compared to the widely used single-level contrastive alignment, imposing multi-level contrastive alignments on both global and local image features contributed to improved segmentation performance.

In the quantitative comparison between our TMCA and state-of-the-art methods (Table 1), language-guided methods leveraging textual guidance, such as Ariadne, EviVLM, and HCFNet, consistently outperformed image-only segmentation methods such as U-Net and U-Net++. We attributed this to the integration of additional textual information that provided location and size related to ROI targets, as exemplified in Figure 3. The results of LViT are relatively lower among language-guided methods, and this is likely due to LViT only employing a simple tokenization layer to extract text features, which limits the ability to capture high-level textual semantics related to segmentation. Ariadne employed a well-pretrained text encoder capable of extracting rich, high-level textual semantics, thereby achieving improved segmentation performance. HCFNet outperformed all other language-guided methods, and we attribute this partly to the use of contrastive learning for aligning image-text patterns. Nevertheless, our TMCA still outperformed HCFNet consistently across all evaluation datasets by introducing target-informed multi-level contrastive alignments to bridge the image-text pattern gaps in a segmentation-tailored manner. With reduced image-text pattern gaps, textual information can be more effectively incorporated for segmentation, as evidenced in Figure 3 showing that our TMCA more precisely employed the textual semantics to guide segmentation in hard negative cases. In addition, despite the fact that most of the compared methods exhibited inconsistent performance across different datasets, we found that HCFNet and our TMCA achieved consistently better performance than other segmentation methods. This implies that contrastive alignments might enhance the model’s generalizability to different

imaging modalities, likely because the pattern discrepancies across imaging modalities can be alleviated by aligning image features with the textual semantics of unified natural language descriptions.

In the ablation analysis of each technical component (Table 2), employing standard contrastive alignments with MCAS has already yielded superior segmentation performance over the baseline model, while adding LTEM and TSDM further enhanced the performance. Existing contrastive alignment techniques align the entire image and text holistically, which incurs difficulties in aligning images and text with semantic similarities merely in disease-related regions and inevitably introduces false negatives during alignments. Moreover, in medical images, important information could only occupy a small portion of the image. This subtle yet critical information may be overlooked by excessive non-critical normal or background information. Our TSDM calculates the semantic distance based on the interaction of ground truth segmentation masks, which enables the focus on critical disease-related information in contrastive alignment modeling. Additionally, with image-text features aligned, our LTEM identifies critical image regions through cross-attention from the text on the image and then reinforces these regions, which aligns with the widely used spatial attention mechanism [45] and has been proven beneficial for accurate segmentation in our experiments.

In the ablation analysis on multi-level contrastive alignments (Table 3), our TMCA yielded larger improvements when more levels of contrastive alignments were applied. We suggest that this is because, with contrastive alignments applied at higher-scale image features, finer-grained textual guidance is integrated with more detailed image contexts for accurate segmentation. When only the global text and image features at the deepest layer are aligned via contrastive alignment, information integration at shallower layers may become confused and distract the decoder’s features from important regions. These shallow layers, which focus on local image details such as the ROI boundaries, are heavily reliant on high-level image semantics and auxiliary textual guidance to identify attentive regions. By incorporating contrastive alignments at multiple pyramid levels, our TMCA can leverage textual semantics to directly guide the modeling of local image details. This approach also enables our LTEM, which associates each image sub-region with text by calculating the feature similarities, to provide more accurate localization guidance at multiple pyramid levels. This is particularly important when the ROI targets are small and primarily rely on subtle image details to identify. Intuitively, this observation is also consistent with deep supervision, where additional auxiliary supervision provides supplementary guidance on the intermediate modeling of neural networks [46, 47].

Language-guided medical image segmentation has proven useful in practical scenarios where clinicians can provide interactive language guidance [6] and also in retrospective studies where image-text pairs are readily available, as in this study. A key limitation is that existing works relied on the text inputs that were carefully crafted by humans to be concise and direct for describing ROIs (e.g., “one small brown oval polyp, located in the top right of the image”). In routine clinical workflows, however, medical reports can be much longer, including important information such as patient history, scanning protocols, relationships to adjacent organs, and details about the lack of involvement of other organs/structures. Such reports pose challenges to language-guided segmentation methods as their textual semantics are implicit and can be difficult to extract. This may be mitigated by recent natural language processing (NLP) techniques, for example, lengthy textual reports can be refined and structured using large language models (LLMs) [48, 49]. As future work, we will investigate the use of LLM to process such clinical imaging reports and evaluate its performance with our TMCA. We will also curate segmentation datasets containing more complex clinical reports. Also, we will explore language-guided segmentation for 3D medical images, which is more complicated and requires finer-grained textual guidance.

7. Conclusion

In this study, we have outlined a Target-informed Multi-level Contrastive Alignment framework (TMCA) for language-guided medical image segmentation, which bridges the inherent image-text pattern gaps to optimize cross-modal information integration through multi-level fine-grained target-sensitive contrastive alignments. Our TMCA introduces a Target-sensitive Semantic Distance Module (TSDM) and a Language-guided Target Enhancement Module (LTEM) to deliver finer-grained textual guidance for critical

image regions, and also introduces a Multi-level Contrastive Alignment Strategy (MCAS) to direct textual guidance to multi-scale image features with rich image details. Extensive experiments demonstrated that our TMCA consistently outperformed state-of-the-art medical image segmentation methods across four well-established benchmark datasets and thus exhibited good generalizability across various segmentation tasks and medical imaging modalities.

Acknowledgements

This work was supported in part by Australian Research Council (ARC) grant DP200103748.

References

- [1] Chen, Xuxin, Ximin Wang, Ke Zhang, Kar-Ming Fung, Theresa C. Thai, Kathleen Moore, Robert S. Mannel, Hong Liu, Bin Zheng, and Yuchen Qiu. "Recent advances and clinical applications of deep learning in medical image analysis." *Medical image analysis* 79 (2022): 102444. <https://doi.org/10.1016/j.media.2022.102444>.
- [2] Jiang, Xiaoyan, Zuojin Hu, Shuihua Wang, and Yudong Zhang. "Deep learning for medical image-based cancer diagnosis." *Cancers* 15, no. 14 (2023): 3608. <https://doi.org/10.3390/cancers15143608>.
- [3] Wang, Risheng, Tao Lei, Ruixia Cui, Bingtao Zhang, Hongying Meng, and Asoke K. Nandi. "Medical image segmentation using deep learning: A survey." *IET image processing* 16, no. 5 (2022): 1243-1267. <https://doi.org/10.1049/ipr2.12419>.
- [4] Li, Yuanyuan, Yifei Duan, Guanqiu Qi, Baisen Cong, Li Zhang, and Zhiqin Zhu. "A Lightweight Vision Mamba Coding UNet for medical image segmentation." *Engineering Applications of Artificial Intelligence* 162 (2025): 112676. <https://doi.org/10.1016/j.engappai.2025.112676>.
- [5] Tan, Dayu, Manman Shi, Yansen Su, Xin Peng, Chunhou Zheng, Kaixun He, and Weimin Zhong. "An efficient and lightweight adaptive network for three-dimensional medical image segmentation." *Engineering Applications of Artificial Intelligence* 160 (2025): 111999. <https://doi.org/10.1016/j.engappai.2025.111999>.
- [6] Li, Zihan, Yunxiang Li, Qingde Li, Puyang Wang, et al. "Lvit: language meets vision transformer in medical image segmentation." *IEEE transactions on medical imaging* 43, no. 1 (2023): 96-107. <https://doi.org/10.1109/TMI.2023.3291719>.
- [7] Zhong, Yi, Mengqiu Xu, Kongming Liang, Kaixin Chen, and Ming Wu. "Ariadne's thread: Using text prompts to improve segmentation of infected areas from chest x-ray images." In *International Conference on Medical Image Computing and Computer-Assisted Intervention*, pp. 724-733. Cham: Springer Nature Switzerland, 2023. https://doi.org/10.1007/978-3-031-43901-8_69.
- [8] Lee, Go-Eun, Seon Ho Kim, Jungchan Cho, Sang Tae Choi, and Sang-Il Choi. "Text-guided cross-position attention for segmentation: Case of medical image." In *International Conference on Medical Image Computing and Computer-Assisted Intervention*, pp. 537-546. Cham: Springer Nature Switzerland, 2023. https://doi.org/10.1007/978-3-031-43904-9_52.
- [9] Tomar, Nikhil Kumar, Debesh Jha, Ulas Bagci, and Sharib Ali. "TGANet: Text-guided attention for improved polyp segmentation." In *International Conference on Medical Image Computing and Computer-Assisted Intervention*, pp. 151-160. Cham: Springer Nature Switzerland, 2022. https://doi.org/10.1007/978-3-031-16437-8_15.
- [10] Zhang, Yuhao, Hang Jiang, Yasuhide Miura, Christopher D. Manning, and Curtis P. Langlotz. "Contrastive learning of medical visual representations from paired images and text." In *Machine learning for healthcare conference*, pp. 2-25. PMLR, 2022.
- [11] Zhao, Zihao, Yuxiao Liu, Han Wu, Mei Wang, Yonghao Li, Sheng Wang, Lin Teng et al. "Clip in medical imaging: A comprehensive survey." *arXiv preprint arXiv:2312.07353* (2023). <https://doi.org/10.48550/arXiv.2312.07353>.
- [12] Degerli, Aysen, Serkan Kiranyaz, Muhammad EH Chowdhury, and Moncef Gabbouj. "Osegnet: Operational segmentation network for covid-19 detection using chest x-ray images." In *2022 IEEE International Conference on Image Processing (ICIP)*, pp. 2306-2310. IEEE, 2022. <https://doi.org/10.1109/ICIP46576.2022.9897412>.
- [13] Morozov, Sergey P., Anna E. Andreychenko, Nikolay A. Pavlov, A. V. Vladzimyrskyy, Natalya V. Ledikhova, Victor A. Gombolevskiy, Ivan A. Blokhin, Pavel B. Gelezhe, A. V. Gonchar, and V. Yu Chernina. "Mosmeddata: Chest ct scans with covid-19 related findings dataset." *arXiv preprint arXiv:2005.06465* (2020). <http://arxiv.org/abs/2005.06465>.
- [14] Jha, Debesh, Pia H. Smedsrød, Michael A. Riegler, Pål Halvorsen, Thomas De Lange, Dag Johansen, and Håvard D. Johansen. "Kvasir-seg: A segmented polyp dataset." In *International conference on multimedia modeling*, pp. 451-462. Cham: Springer International Publishing, 2019. https://doi.org/10.1007/978-3-030-37734-2_37.
- [15] Ngoc Lan, Phan, Nguyen Sy An, Dao Viet Hang, Dao Van Long, Tran Quang Trung, Nguyen Thi Thuy, and Dinh Viet Sang. "Neounet: Towards accurate colon polyp segmentation and neoplasm detection." In *International Symposium on Visual Computing*, pp. 15-28. Cham: Springer International Publishing, 2021. https://doi.org/10.1007/978-3-030-90436-4_2.
- [16] Ronneberger, Olaf, Philipp Fischer, and Thomas Brox. "U-net: Convolutional networks for biomedical image segmentation." In *International Conference on Medical image computing and computer-assisted intervention*, pp. 234-241. Cham: Springer international publishing, 2015. https://doi.org/10.1007/978-3-319-24574-4_28.
- [17] Zhou, Zongwei, Md Mahfuzur Rahman Siddiquee, Nima Tajbakhsh, and Jianming Liang. "Unet++: A nested u-net architecture for medical image segmentation." In *International workshop on deep learning in medical image analysis*, pp. 3-11. Cham: Springer International Publishing, 2018. https://doi.org/10.1007/978-3-030-00889-5_1.
- [18] Oktay, Ozan, Jo Schlemper, Loic Le Folgoc, Matthew Lee, Mattias Heinrich, Kazunari Misawa, Kensaku Mori et al. "Attention u-net: Learning where to look for the pancreas." *arXiv preprint arXiv:1804.03999* (2018). <https://doi.org/10.48550/arXiv.1804.03999>.

[19] Hatamizadeh, Ali, Vishwesh Nath, Yucheng Tang, Dong Yang, Holger R. Roth, and Daguang Xu. "Swin unetr: Swin transformers for semantic segmentation of brain tumors in mri images." In International MICCAI brainlesion workshop, pp. 272-284. Cham: Springer International Publishing, 2021. https://doi.org/10.1007/978-3-031-08999-2_22.

[20] F. Isensee, P.F. Jaeger, S.A. Kohl, J. Petersen, K.H. Maier-Hein, nnU-Net: a self-configuring method for deep learning-based biomedical image segmentation, *Nature Methods* 18 (2021) 203-211. <https://doi.org/10.1038/s41592-020-01008-z>.

[21] Ma, Jun, Yuting He, Feifei Li, Lin Han, Chenyu You, and Bo Wang. "Segment anything in medical images." *Nature Communications* 15, no. 1 (2024): 654. <https://doi.org/10.1038/s41467-024-44824-z>.

[22] Ma, Jun, Zongxin Yang, Sumin Kim, Bihui Chen, et al. "Medsam2: Segment anything in 3d medical images and videos." *arXiv preprint arXiv:2504.03600* (2025). <https://doi.org/10.48550/arXiv.2504.03600>.

[23] Kammitsas, Konstantinos, Wenjia Bai, Enzo Ferrante, Steven McDonagh, Matthew Sinclair, Nick Pawlowski, Martin Rajchl et al. "Ensembles of multiple models and architectures for robust brain tumour segmentation." In International MICCAI brainlesion workshop, pp. 450-462. Cham: Springer International Publishing, 2017. https://doi.org/10.1007/978-3-319-75238-9_38.

[24] Guo, Zhe, Xiang Li, Heng Huang, Ning Guo, and Quanzheng Li. "Deep learning-based image segmentation on multimodal medical imaging." *IEEE transactions on radiation and plasma medical sciences* 3, no. 2 (2019): 162-169. <https://doi.org/10.1109/TRPMS.2018.2890359>.

[25] Shen, Dinggang, Guorong Wu, and Heung-Il Suk. "Deep learning in medical image analysis." *Annual review of biomedical engineering* 19, no. 1 (2017): 221-248. <https://doi.org/10.1146/annurev-bioeng-071516-044442>.

[26] Dosovitskiy, Alexey, Lucas Beyer, Alexander Kolesnikov, Dirk Weissenborn, Xiaohua Zhai, Thomas Unterthiner, Mostafa Dehghani et al. "An Image is Worth 16x16 Words: Transformers for Image Recognition at Scale." In *International Conference on Learning Representations*. <https://openreview.net/forum?id=YicbFdNTTy>.

[27] Radford, Alec, Jong Wook Kim, Chris Hallacy, Aditya Ramesh, Gabriel Goh, Sandhini Agarwal, Girish Sastry et al. "Learning transferable visual models from natural language supervision." In *International conference on machine learning*, pp. 8748-8763. PMLR, 2021. <http://arxiv.org/abs/2103.00020>.

[28] Hu, Jihong, Yinhao Li, Hao Sun, Yu Song, Chujie Zhang, Lanfen Lin, and Yen-Wei Chen. "Lga: A language guide adapter for advancing the sam model's capabilities in medical image segmentation." In *International Conference on Medical Image Computing and Computer-Assisted Intervention*, pp. 610-620. Cham: Springer Nature Switzerland, 2024. https://doi.org/10.1007/978-3-031-72390-2_57.

[29] Kirillov, Alexander, Eric Mintun, Nikhila Ravi, Hanzi Mao, Chloe Rolland, Laura Gustafson, Tete Xiao et al. "Segment anything." In *Proceedings of the IEEE/CVF international conference on computer vision*, pp. 4015-4026. 2023.

[30] Devlin, Jacob, Ming-Wei Chang, Kenton Lee, and Kristina Toutanova. "Bert: Pre-training of deep bidirectional transformers for language understanding." In *Proceedings of the 2019 conference of the North American chapter of the association for computational linguistics: human language technologies*, volume 1 (long and short papers), pp. 4171-4186. 2019. <https://doi.org/10.18653/v1/N19-1423>.

[31] Boecking, Benedikt, Naoto Usuyama, Shruthi Bannur, Daniel C. Castro, Anton Schwaighofer, Stephanie Hyland, Maria Wetscherek et al. "Making the most of text semantics to improve biomedical vision–language processing." In *European conference on computer vision*, pp. 1-21. Cham: Springer Nature Switzerland, 2022.

[32] Huang, Xiaoshuang, Hongxiang Li, Meng Cao, Long Chen, et al. "Cross-modal conditioned reconstruction for language-guided medical image segmentation." *IEEE Transactions on Medical Imaging* 44, no. 4 (2025): 1821-1835. <https://doi.org/10.1109/TMI.2024.3523333>.

[33] Ye, Shuchang, Mingyuan Meng, Mingjian Li, Dagan Feng, and Jinman Kim. "Enabling Text-free Inference in Language-guided Segmentation of Chest X-rays via Self-guidance." In *International Conference on Medical Image Computing and Computer-Assisted Intervention*, pp. 242-252. Cham: Springer Nature Switzerland, 2024. https://doi.org/10.1007/978-3-031-72111-3_23.

[34] Ye, Shuchang, Usman Naseem, Mingyuan Meng, and Jinman Kim. "Alleviating Textual Reliance in Medical Language-guided Segmentation via Prototype-driven Semantic Approximation." In *Proceedings of the IEEE/CVF International Conference on Computer Vision*, pp. 22316-22326. 2025.

[35] Pan, Qingtao, Zhengrong Li, Guang Yang, Qing Yang, and Bing Ji. "EviVLM: When Evidential Learning Meets Vision Language Model for Medical Image Segmentation." *IEEE Transactions on Medical Imaging*, early access (2025). <https://doi.org/10.1109/TMI.2025.3622492>.

[36] Zhou, Xichuan, Qianqian Song, Jing Nie, Yujie Feng, Haijun Liu, Fu Liang, Lihui Chen, and Jin Xie. "Hybrid cross-modality fusion network for medical image segmentation with contrastive learning." *Engineering Applications of Artificial Intelligence* 144 (2025): 110073. <https://doi.org/10.1016/j.engappai.2025.110073>.

[37] Huang, Shih-Cheng, Liyue Shen, Matthew P. Lungren, and Serena Yeung. "Gloria: A multimodal global-local representation learning framework for label-efficient medical image recognition." In *Proceedings of the IEEE/CVF international conference on computer vision*, pp. 3942-3951. 2021.

[38] Wang, Fuying, Yuyin Zhou, Shujun Wang, Varut Vardhanabutti, and Lequan Yu. "Multi-granularity cross-modal alignment for generalized medical visual representation learning." *Advances in neural information processing systems* 35 (2022): 33536-33549.

[39] Li, Mingjian, Mingyuan Meng, Michael Fulham, David Dagan Feng, Lei Bi, and Jinman Kim. "Enhancing medical vision-language contrastive learning via inter-matching relation modelling." *IEEE Transactions on Medical Imaging* (2025). <https://doi.org/10.1109/TMI.2025.3534436>.

[40] Wang, Zifeng, Zhenbang Wu, Dinesh Agarwal, and Jimeng Sun. "Medclip: Contrastive learning from unpaired medical images and text." In *Proceedings of the Conference on Empirical Methods in Natural Language Processing*. Conference on Empirical Methods in Natural Language Processing, vol. 2022, p. 3876. 2022. <https://doi.org/10.18653/v1/2022.emnlp-main.256>.

[41] Liu, Bo, Donghuan Lu, Dong Wei, Xian Wu, Yan Wang, Yu Zhang, and Yefeng Zheng. "Improving medical vision-language contrastive pretraining with semantics-aware triage." *IEEE Transactions on Medical Imaging* 42, no. 12 (2023): 3579-3589. <https://doi.org/10.1109/TMI.2023.3294980>.

[42] Liu, Zhuang, Hanzi Mao, Chao-Yuan Wu, Christoph Feichtenhofer, Trevor Darrell, and Saining Xie. "A convnet for the 2020s." In *Proceedings of the IEEE/CVF conference on computer vision and pattern recognition*, pp. 11976-11986. 2022.

[43] Selvaraju, Ramprasaath R., Michael Cogswell, Abhishek Das, Ramakrishna Vedantam, Devi Parikh, and Dhruv Batra. "Grad-cam: Visual explanations from deep networks via gradient-based localization." In Proceedings of the IEEE international conference on computer vision, pp. 618-626. 2017. <https://doi.org/10.1007/s11263-019-01228-7>.

[44] Poudel, Kanchan, Manish Dhakal, Prasiddha Bhandari, Rabin Adhikari, Safal Thapaliya, and Bishesh Khanal. "Exploring transfer learning in medical image segmentation using vision-language models." arXiv preprint arXiv:2308.07706 (2023). <https://doi.org/10.48550/arXiv.2308.07706>.

[45] Hu, Jie, Li Shen, and Gang Sun. "Squeeze-and-excitation networks." In Proceedings of the IEEE conference on computer vision and pattern recognition, pp. 7132-7141. 2018.

[46] Le'Clerc Arrastia, Jean, Nick Heilenkötter, Daniel Otero Baguer, Lena Hauberg-Lotte, Tobias Boskamp, Sonja Hetzer, Nicole Duschner, Jörg Schaller, and Peter Maass. "Deeply supervised UNet for semantic segmentation to assist dermatopathological assessment of basal cell carcinoma." Journal of imaging 7, no. 4 (2021): 71. <https://doi.org/10.3390/jimaging7040071>.

[47] Zhao, Ziyuan, Zeng Zeng, Kaixin Xu, Cen Chen, and Cuntai Guan. "Dsal: Deeply supervised active learning from strong and weak labelers for biomedical image segmentation." IEEE journal of biomedical and health informatics 25, no. 10 (2021): 3744-3751. <https://doi.org/10.1109/JBHI.2021.3052320>.

[48] Touvron, Hugo, Thibaut Lavril, Gautier Izacard, Xavier Martinet, Marie-Anne Lachaux, Timothée Lacroix, Baptiste Rozière et al. "Llama: Open and efficient foundation language models." arXiv preprint arXiv:2302.13971 (2023). <http://arxiv.org/abs/2302.13971>.

[49] Wu, Chaoyi, Weixiong Lin, Xiaoman Zhang, Ya Zhang, Weidi Xie, and Yanfeng Wang. "PMC-LLaMA: toward building open-source language models for medicine." Journal of the American Medical Informatics Association 31, no. 9 (2024): 1833-1843. <https://doi.org/10.1093/jamia/ocae045>.

[50] Meng, Mingyuan, Yuxin Xue, Dagan Feng, Lei Bi, and Jinman Kim. "Full-resolution MLPs Empower Medical Dense Prediction." arXiv preprint arXiv:2311.16707 (2023). <https://doi.org/10.48550/arXiv.2311.16707>.